DISTRIBUTED APERTURE RADAR TOMOGRAPHIC SENSORS (DARTS) TO MAP SURFACE TOPOGRAPHY AND VEGETATION STRUCTURE

Marco Lavalle[a], Ilgin Seker[a], James Ragan[b], Eric Loria[a], Razi Ahmed[a], Brian P. Hawkins[a], Samuel Prager[a], Duane Clark[a], Robert Beauchamp[a], Mark Haynes[a], Paolo Focardi[a], Nacer Chahat[a], Matthew Anderson[b], Kai Matsuka[b], Vincenzo Capuano[b], Soon-Jo Chung[a, b]

(a) Jet Propulsion Laboratory, California Institute of Technology, 4800 Oak Grove Dr, Pasadena, CA 91109
(b) California Institute of Technology, 1200 E California Blvd, Pasadena, CA 91125

ABSTRACT

Distributed Aperture Radar Tomographic Sensors (DARTS) is a mission concept being studied at the NASA Jet Propulsion Laboratory in collaboration with the California Institute of Technology to enable global and repeated imaging of surface topography and three-dimensional vegetation structure using single-pass tomographic SAR technique. The observing system consists of a distributed formation of multiple small synthetic aperture radar platforms deployed in space with variable distances to achieve look angle diversity and sensitivity to the vertical distribution of vegetation components. Our goal is to identify the optimal system configuration starting from documented community needs and mature the critical technologies that lead to a viable implementation of DARTS. Here, we provide an overview of DARTS and describe our approach for designing and demonstrating single-pass SAR tomographic systems as part of an on-going funded NASA Instrument Incubator Program effort.

Index Terms— Tomography, SAR, topography, vegetation structure.

1. INTRODUCTION

The recent report from the 2017-2027 Decadal Survey for Earth Science and Applications from Space recommended mapping of surface topography and vegetation (STV) structure as one of the high-priority incubator measurements to undertake in the next decade. In response to the 2017-2027 Decadal Survey, the National Aeronautics and Space Administration (NASA) conducted a 1-year study to consult the science community and identify product needs and technology gaps for measuring STV from space. The study generated a set of desired product characteristics for each discipline (solid Earth, cryosphere, ecosystems, hydrology, coastal, and applications). Tab. 1 reports the median values of these characteristics averaged across all disciplines and the median values associated to ecosystem science only. Parameters are further classified between *aspirational* and *threshold* depending on whether they lead to a dramatic or important science advancement. The study reveals that an STV mission should generate global products with weekly cadence for 3-9 years at meter-level horizontal and vertical resolutions in order to address the aspirational needs of all scientific disciplines.

Parameter of final product	All disciplines		Ecosystems	
	Aspir.	Thres.	Aspir.	Thres.
Coverage [%]	90	55	80	50
Repeat frequency [months]	0.2	3	3	12
Horizontal resolution [m]	1	30	30	80
Veg. vertical resolution [m]	1	2	1	2
Vertical accuracy [m]	0.2	0.5	1	2
Bathymetry max. depth [m]	25	10	–	–
Geolocation accuracy [m]	1	5	1	3
Rate change accuracy [cm/y]	10	35	50	200
Duration [years]	9	3	6	3
Latency [days]	5	90	5	30

Table 1. Aspirational and threshold surface topography and vegetation (STV) product needs identified by the NASA 2020 STV Decadal Survey Incubator Study. Median values are reported for all scientific disciplines (solid Earth, cryosphere, ecosystems, hydrology, coastal and applications) and ecosystem science only.

Recent advances in radar techniques have shown that multiple and simultaneous synthetic aperture radar (SAR) observations from different look angles operating in interferometric or tomographic mode can provide high-resolution, gap-free maps of 3D vegetation structure and underlying topography robust to temporal decorrelation [1, 2]. We call such systems Distributed Aperture Radar Tomographic Sensors, or DARTS, as they are characterized by distributed formations of radar platforms operating with a certain level of coordination to achieve the desired STV product characteristics and accuracy. In this paper, we provide an overview of a recently-funded NASA Instrument Incubator Program (IIP) project that aims to mature and demonstrate the key technologies that enable DARTS, and discuss an example of integrated trade study for the design of the optimal orbital configuration of the distributed SAR formation for mapping STV.

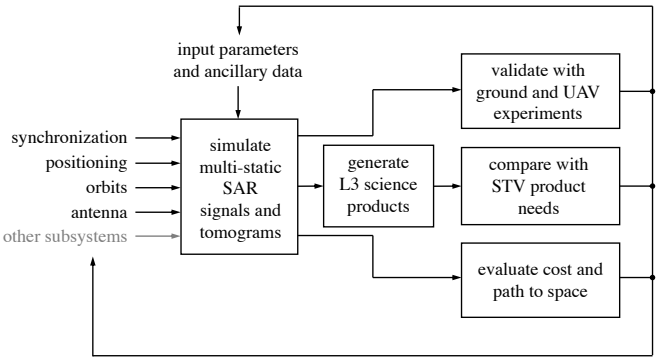

Fig. 1. High-level approach to the design and demonstration of the Distributed Aperture Radar Tomographic Sensors (DARTS) concept.

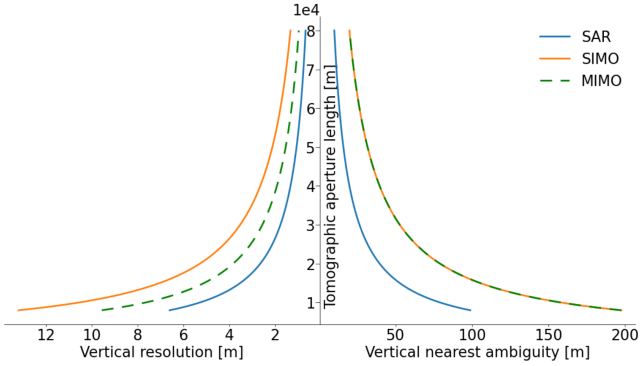

Fig. 2. Vertical resolution δ_z and vertical nearest ambiguity A_z^1 as a function of the tomographic aperture length L for three multi-static modes (SAR, SIMO, and full MIMO) for 15 platforms.

2. DESIGN AND DEMONSTRATION OF DARTS

The design of distributed formations with an arbitrary number of radar platforms that can meet a given set of science objectives is not straightforward due to the complexity of the trade space as well as the low maturity of some of the critical technologies. While the larger number of degrees of freedom allows for more flexibility compared to the case of single-platform or tandem systems, the competing trade-offs coupled with the unknown performance of the various technologies under development make the design a highly iterative and challenging process.

A formation with N_L platforms equipped with L-band radars, for instance, may provide comparable performance to a formation with $N_S > N_L$ platforms equipped with S-band radars, with the advantage that radar electronics and antenna subsystem at higher frequencies would be more compact and consume less power. Similarly, adopting a different tomographic focusing algorithm may lead to different performance depending on the radar frequency and number of platforms, which in turn may affect the optimal orbital configuration and the required performance of the signal synchronization and positioning algorithms for ensuring phase coherency in the tomographic focusing.

For DARTS, we focus on the maturation, integration, and demonstration of: 1) Absolute timing reference that is invariant to positioning of the platforms; 2) relative positioning and attitude knowledge in three dimensions for all platforms; 3) intercommunication and assimilation of each radar's data for coherent data processing; 4) miniaturized, lightweight radar components conducive to affordable launch of multi-satellite formations; 5) lightweight and deployable antenna; 6) optimal orbital and multi-static radar mode configuration; 7) conversion of SAR tomograms into L3 science products; and 8) validation of system performance with prototype hardware.

The central element in the design of DARTS is a trade study tool (TST) that combines high-fidelity multi-baseline interferometric and tomographic SAR (TomoSAR) simulations informed by state-of-the-art algorithms and technologies with demonstrated performance. Simulations are converted into higher-level STV science metrics listed in Tab. 1 in order to guide the exploration of the trade space. The high-level block diagram of the TST is illustrated in Fig. 1. Hardware demonstration and validation of DARTS are conducted both on the ground through in-lab tests and in-air using uninhabited aerial vehicles (UAVs). A separate IGARSS2021 paper is available with focus on phase synchronization and UAV experiments in support of DARTS [3]. Hardware implementation is currently underway with commercial-off-the-shelf hardware and RF system-on-chip (RFSoC), which enable both compact radar architectures as well as flexibility. Where feasible, the key technologies are implemented using RFSoC to reduce size, mass, power, and cost and enable eventual deployment on small satellites.

3. EXAMPLE OF TRADE STUDY: TOMOSAR FORMATION DESIGN AND OPTIMIZATION

Our initial trade studies focused on the effects of the multi-static modes on tomographic resolution and ambiguity, and on the design of optimal orbits for TomoSAR assuming no synchronization and positioning errors [4]. Three multi-static modes have been analyzed and compared so far: SAR (or ping-pong), where each platform transmits/receives sequentially as in traditional along-track SAR; (2) SIMO (single-input multiple-output), where a single platform transmits and all platforms receive; and (3) full MIMO (multiple-input multiple-output), where multiple platforms transmit sequentially and multiple platforms receive simultaneously for each transmit platform [5]. We use the equations of TomoSAR resolution and ambiguity, as well as the numerical ISLR computation, to constrain and optimize the orbital trajectories in a distributed formation [6]. Assuming rectilinear and uniform platform distribution, the tomographic resolution δ_z and

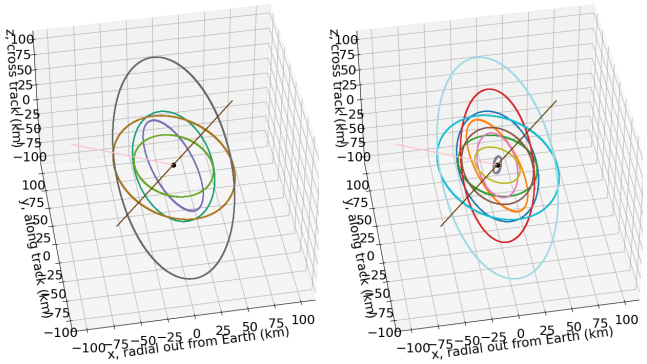

Fig. 3. 3D view of the distributed formation with 6 (left) and 12 (right) spacecraft on J_2-perturbed dynamic orbits in the LVLH frame. The black dot is the chief satellite. The radar line of sight (pink) and baseline (brown) are also shown.

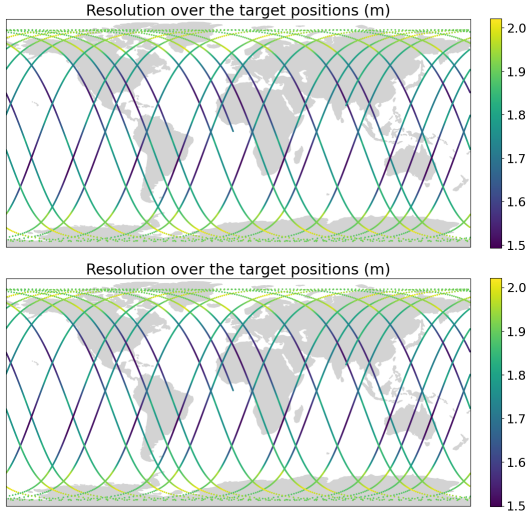

Fig. 4. Tomographic resolution for formations with 6 (top) and 12 (bottom) satellites both satisfying the given resolution constraint $\delta_z < 2\,\mathrm{m}$.

the nearest ambiguity location A_z^1 along the vertical direction z for flat earth can be written as [7],

$$\delta_z = \frac{w_n \lambda H \tan\theta}{p_\delta L \cos\left(|\theta - \alpha|\right)} \tag{1}$$

and

$$A_z^1 = \frac{\lambda H \tan\theta}{p_a \mu \cos\left(|\theta - \alpha|\right)} \tag{2}$$

where λ is the radar wavelength, H is the formation altitude above the Earth's surface, L is the tomographic aperture length, μ is the platform spacing, θ is the look angle, α is the baseline orientation angle, w_n the expansion coefficient due to windowing to reduce sidelobes, and p_δ and p_a are coefficients that account for the multi-static mode

$$\begin{aligned} \text{SAR:}\ & p_\delta = p_a = 2 \\ \text{SIMO:}\ & p_\delta = p_a = 1 \\ \text{MIMO:}\ & p_\delta \simeq 1.38,\ p_a = 1 \end{aligned}$$

The tomographic aperture length can be obtained by adding one platform spacing to the maximum distance between the platforms, i.e., $L = (N-1)\mu + \mu = N\mu$, where N is the number of platforms [7]. Note that (1) assumes that the range bandwidth is sufficiently large, and therefore the greater axis of the tomographic resolution cell is oriented along the direction perpendicular to the look direction. Fig. 2 shows how (1) and (2) change as a function of the multi-static mode and the tomographic aperture length L for $N = 15$ platforms. To achieve a vertical resolution of 2 m as listed in Tab. 1, for instance, the SAR mode requires a smaller aperture length compared to SIMO and MIMO modes, but translates into a smaller vertical ambiguity location.

Because platforms in a realistic formation are not uniformly distributed, target replicas are smeared out along the direction perpendicular to slant range [7]. For this reason, the integrated side-lobe ratio (ISLR) is typically a better metric than ambiguity location to evaluate the quality of the TomoSAR measurements. In our trade study, the ISLR is calculated from the ratio between the integrated energy of the side lobes of the tomographic point spread function and the integrated energy of the 4-dB main lobe. The tomographic point spread function is simulated using time-domain backprojection along the direction perpendicular to slant range for the scene extent using platform locations, look angle, local slope, maximum target height, and radar frequency, and depends on the multi-static mode.

The decision variable of this optimization problem is the passive relative orbit (PRO) selected for the formation. PROs are a particularly suitable framework for designing formation flying mission orbits because PROs are constructed to match the orbital energy of each platform in a formation (i.e., the energy of a *deputy* matching that of the reference (*chief*) satellite, resulting in a formation that minimizes drift even in the presence of J_2 disturbance [8]. This is desirable as a bounded formation minimizes drift and fuel costs. The optimization algorithm takes a set of initial orbital positions for each platform $\mathbf{x}_0$ from which velocities are computed via the energy matching condition in order to follow J_2-invariant PROs using equations provided in [8]. The initial positions and velocities are then propagated to compute the relative trajectories as function of time and evaluated against the objective function $F(\mathbf{x}_0)$ of the form [6]

$$F(\mathbf{x}_0) = F_f(\mathbf{x}_0) + \alpha F_s(\mathbf{x}_0) = F_f(\mathbf{x}_0) + \alpha \int_{t_0}^{t_1} M(\mathbf{x}_0, \tau)\, \mathrm{d}\tau \tag{3}$$

where $F_f(\mathbf{x}_0)$ is the fuel penalty model and $F_s(\mathbf{x}_0)$ is the TomoSAR-specific science objective model and α is a relative weighting parameter between the two objective compo-

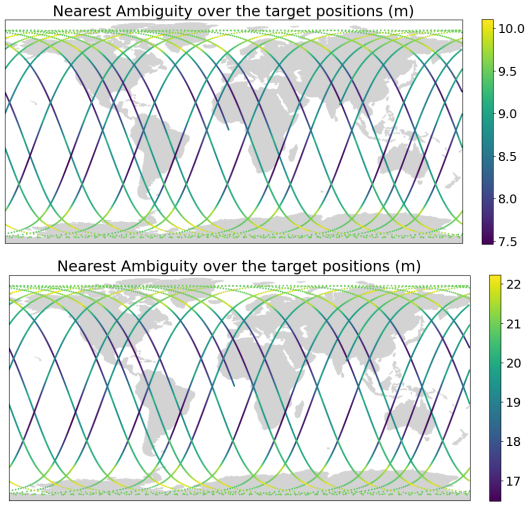

Fig. 5. Tomographic nearest ambiguity location for optimized formations with 6 (top) and 12 (bottom) spacecrafts.

nents. By tuning the objective models for both the fuel cost and the scientific merit over multiple orbits to match the mission priorities, we can not only quantify the tomographic performance of a given formation, but also derive the optimal formation PROs given input mission requirements. The science objective $F_s(\mathbf{x}_0)$ can be written as a TomoSAR metric $M(\mathbf{x}_0, \tau)$ (e.g., function of resolution or ambiguity or ISLR) integrated over time τ between the epochs t_0 and t_1 along the orbits (e.g., half a day or longer). In addition to the choice of the science objective function, one can refine the optimization problem by imposing additional inequality constraints, such as that the critical baseline is never exceeded, or that the vertical resolution is always smaller that a given value. A genetic algorithm is employed to solve the orbital optimization problem. The details of the optimization algorithm are given in [6].

Figure 3 illustrates the optimized 3D formations obtained with 6 and 12 satellites. The black dot is the chief satellite and the colored trajectories represent each deputy's orbit. Both formations were designed by setting M as the ISLR subject to the constraint that the resolution be less than 2 m, and using the SAR (ping-pong) tomographic mode with NISAR as a chief orbit. Because vertical resolution in (1) is determined by the maximum tomographic aperture L, the maximum spread of the formation is the same for the 6 and 12 satellites cases. Figure 4 confirms that resolution is always below 2 m with larger values near the poles where orbits are closer to each other. The average distance between the platforms in each formation is 10-14 km and 10-30 km for the 6 and 12 satellite case, respectively. This difference impacts the nearest ambiguity as illustrated in Fig. 5 where the smaller formation with 6 platforms has poorer performance compared with the larger formation. Although not shown here, using the MIMO mode and potentially other metrics for optimization is expected to provide increased overall tomographic performance.

4. CONCLUSION

DARTS is a mission concept under formulation at JPL/Caltech to address the science and application needs of the broad STV community. We have been maturing and integrating the technologies that enable smallsats and distributed SAR formations, which are at the core of DARTS. Integration is ongoing both at software and hardware levels. In this paper, we have provided an example trade study for optimizing the orbital trajectories given a set of tomographic requirements. Future works include the design and demonstration of DARTS after integration of its various subsystems as shown in Fig. 1

5. ACKNOWLEDGMENTS

The research reported here was carried out in part at the Jet Propulsion Laboratory, Caltech, under a contract with the National Aeronautics and Space Administration (80NM0018D0004). We would like to thank ESTO for providing the funds.

6. REFERENCES

[1] A. Reigber and A. Moreira, "First demonstration of airborne SAR tomography using multibaseline L-band data," *IEEE Transactions on Geoscience and Remote Sensing*, vol. 38, no. 5, pp. 2142–2152, Sep. 2000.

[2] A. Moreira, P. Prats-Iraola, M. Younis, G. Krieger, I. Hajnsek, and K. P. Papathanassiou, "A tutorial on synthetic aperture radar," *IEEE Geoscience and Remote Sensing Magazine*, vol. 1, no. 1, pp. 6–43, mar 2013.

[3] B. Hawkins, M. Anderson, S. Prager, S.-J. Chung, and M. Lavalle, "Experiments with small UAS to support SAR tomographic mission formulation," in *2021 IEEE Inter. Geoscience and Remote Sensing Symposium (IGARSS)*, July 2021.

[4] S. Prager, M. S. Haynes, and M. Moghaddam, "Wireless Subnanosecond RF Synchronization for Distributed Ultrawideband Software-Defined Radar Networks," *IEEE Trans. on Microwave Theory and Techniques*, vol. 68, no. 11, pp. 4787–4804, 2020.

[5] G. Krieger, "MIMO-SAR: Opportunities and Pitfalls," *IEEE Transactions on Geoscience and Remote Sensing*, vol. 52, no. 5, pp. 2628–2645, 2014.

[6] J. Ragan, R. Ahmed, K. Matsuka, I. Seker, J. Walker, S.-J. Chung, and M. Lavalle, "Optimizing formation flying orbit design," in *Advances in the Astronautical Sciences*, 2021.

[7] I. Seker and M. Lavalle, "Tomographic performance of multistatic radar formations: Theory and simulations," *Remote Sensing*, vol. 13, no. 4, 2021.

[8] D. Morgan, S.-J. Chung, L. Blackmore, B. Acikmese, D. Bayard, and F. Y. Hadaegh, "Swarm-keeping strategies for spacecraft under j2 and atmospheric drag perturbations," *Journal of Guidance, Control, and Dynamics*, vol. 35, no. 5, pp. 1492–1506, 2012.